A Hill-based computational homogenization approach for effective elastic properties of Kelvin open-cell foams

Wenqi Zhu, Nawfal Blal, Salvatore Cunsolo, Dominique Baillis, Paul-Marie Michaud

CSMA 2017
13ème Colloque National en Calcul des Structures
15-19 Mai 2017, Presqu'île de Giens (Var)

A Hill-based computational homogenization approach for effective elastic properties of Kelvin open-cell foams

W. Zhu[1], N. Blal[1], S. Cunsolo[1], D. Baillis[1], P.M. Michaud[2]

[1] *LaMCoS, INSA Lyon, {wenqi.zhu, nawfal.blal, salvatore.cunsolo, dominique.baillis}@insa-lyon.fr*
[2] *EC2-modélisation, paul-marie.michaud@ec2-modelisation.fr*

Abstract — The aim of this study is to investigate the influences of morphological parameters on the effective elastic properties of Kelvin open-cell foam. To obtain realistic cell structure, a method based on Voronoi partition combined with Surface Evolver is developed with high control of a number of morphological parameters. The periodic computational homogenization approach is used to predict the elastic effective properties. Finally, new generic laws are proposed to approximate the effective elastic properties of Kelvin open-cell foam.
Mots clés — Kelvin open-cell foam, morphology, homogenization, Hill's lemma, elasticity, generic laws.

1 Introduction

Cellular foams are important materials for a wide range of applications due to the excellent combination of mechanical and thermal properties [1, 2]. Their physical properties, especially mechanical properties, are always the popular research topics. However it is expensive to model and compute such structures in the macro-scale because the dimensions of structures and constituents have huge differences [3]. The framework of periodic computational homogenization approaches [4] is used in order to derive the effective properties of the heterogeneous medium.

2 Methodology

2.1 Modeling of Kelvin open-cell structure

A new methodology is proposed to generate realistic foam structures with a number of morphological parameters. The morphology is described with a set of geometrical characteristics. The first one is the foam relative density, ρ^*/ρ^b. Here and in the following, the superscript notations * and ^{b} stand for homogenized and bulk properties receptively. The relative densities of models are focused in the range $[4\% - 14\%]$, which corresponds to actual polymer and metallic foams with good thermal insulation and mechanical properties.

The second parameter represents the variation of the cross-sectional area of a strut along the strut axis. The diameter of the circumcircle of the cross section, $d(\eta)$, is normalized by the value at mid-span, d_{min}, as a function of axial position, $\eta = x/l$:

$$d(\eta) = d_{min}\left[1 + \frac{(1-t)\,(2\eta-1)^2}{t}\right],$$

where x is the local abscissa and l is the length of the strut. The parameter t stands for the ratio of minimum to maximum diameter, denoted diameter ratio, which can be presented as $t = d_{min}/d_{max}$. This parameter, t, could be controlled to obtain different longitudinal profiles of struts as illustrated in Table 1.

The third parameter describes the shape of the cross section of the strut. We consider the cross section is represented as an equilateral triangle whose sides are curved with constant curvature. A parameter k, named normalized curvature, is used to describe the shape of the triangle. It equals to the curvature

radius of the circumcircle of the triangle divided by the curvature radius of the sides. By controlling k, the cross section could be generated from concave triangle to flat triangle and to circle. One can see the variation of cross section in Table 2.

Table 1 – Illustration of the models with different diameter ratios

t	0.33	0.6	1
Models	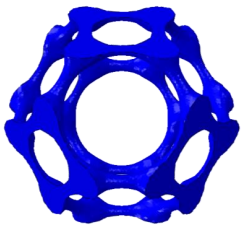	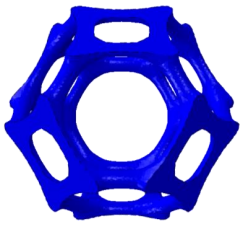	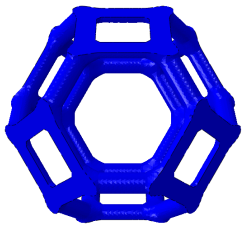

Table 2 – Illustration of the models with different normalized curvatures

k	-0.3	0.25	1
Models	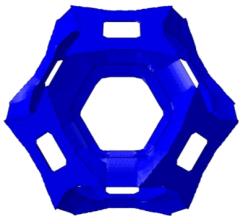	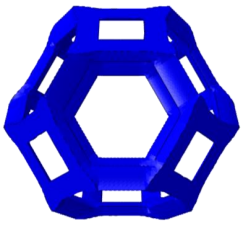	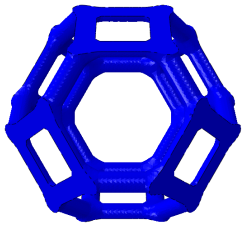

2.2 A Hill's lemma periodic computational homogenization approach

The case of the linearized elasticity with small perturbation is considered herein. For elastic Kelvin open-cell, a representative volume element (RVE) is characterized by the the previous morphological parameters and the local constitutive behavior of the bulk phase, i.e. $\boldsymbol{\sigma}(\boldsymbol{x}) = \mathbb{C}(\boldsymbol{x}) : \boldsymbol{\epsilon}(\boldsymbol{x})$ with $\boldsymbol{\sigma}$ (resp. $\boldsymbol{\epsilon}$) is the local stress (resp. strain) and $\mathbb{C}$ the local fourth-order elasticity tensor in a spatial point $\boldsymbol{x} \in \Omega$. The homogenized behavior over the RVE, given by the effective stiffness tensor $\mathbb{C}^*$, reads in the framework of average fields theory:

$$\overline{\boldsymbol{\sigma}} = \mathbb{C}^* : \overline{\boldsymbol{\epsilon}} \tag{1}$$

where the macroscopic field is given by $\overline{(\bullet)} = \langle \bullet \rangle$ with the average operator defined as $\langle \bullet \rangle = \frac{1}{V} \int_\Omega \bullet \, d\boldsymbol{x}$, V is the volume of the RVE, Ω stands for the solid part. The problem is computationally solved using a periodic homogenization approach. Thus, using modified Voigt notations, the previous homogeneous law Eq. 1 reads: $\{\overline{\boldsymbol{\sigma}}\} = [C^*]\{\overline{\boldsymbol{\epsilon}}\}$ ($\{\bullet\}$ and $[\bullet]$ stand for vectorial and matrix notations of the considered tensors).

According to the Hill's lemma for periodic media [4], the finite element discretization of the problem consists in solving the system [5]:

$$\begin{cases} [\boldsymbol{K}]\{\boldsymbol{u'}\} + [\boldsymbol{F}]\{\overline{\boldsymbol{\epsilon}}\} = \{\boldsymbol{0}\} \\ {}^T[\boldsymbol{F}]\{\boldsymbol{u'}\} + \langle [\boldsymbol{C}] \rangle \{\overline{\boldsymbol{\epsilon}}\} = \{\overline{\boldsymbol{\sigma}}\} \end{cases}, \tag{2}$$

with $\{\boldsymbol{u'}\}$ is fluctuation periodic displacements vector, and the finite element discretized matrices are

given by:

$$\begin{cases} \langle [\boldsymbol{C}] \rangle = \dfrac{1}{V} \displaystyle\int_{\Omega} [\boldsymbol{C}] d\boldsymbol{x}, \\ [\boldsymbol{F}] = \dfrac{1}{V} \displaystyle\int_{\Omega} [\boldsymbol{B}]^T [\boldsymbol{C}] d\boldsymbol{x} \\ [\boldsymbol{K}] = \dfrac{1}{V} \displaystyle\int_{\Omega} [\boldsymbol{B}]^T [\boldsymbol{C}] [\boldsymbol{B}] d\boldsymbol{x}, \end{cases} \tag{3}$$

where $[\boldsymbol{B}]$ is the matrix relating strains and displacements. The periodic boundary condition are taken into account using the selection operator for the opposite nodes over boundaries $[\boldsymbol{\Pi}]$, namely:

$$[\boldsymbol{\Pi}]\{\boldsymbol{u'}\} = \{\boldsymbol{0}\}, \tag{4}$$

Inspirited by the method VAMUCH [1] recently presented in [6] , we propose to solve the system Eq. 2 without imposing six elementary macro-strains or macro-stresses as boundary conditions, which are usually essential for previous finite element methods [7, 8]. Indeed, Eq. $2_{(1)}$ could be written as

$$[\boldsymbol{K}]\{\boldsymbol{u'}\} = -[\boldsymbol{F}]\{\bar{\boldsymbol{\epsilon}}\} \quad \text{under the periodicity constraint} \quad [\boldsymbol{\Pi}]\{\boldsymbol{u'}\} = \{\boldsymbol{0}\}.$$

This equation clearly shows that the fluctuation displacement field $\{\boldsymbol{u'}\}$ linearly depends on $\{\bar{\boldsymbol{\epsilon}}\}$:

$$\{\boldsymbol{u'}\} = [\boldsymbol{M}]\{\bar{\boldsymbol{\epsilon}}\}, \tag{5}$$

where $[\boldsymbol{M}]$ is a macroscopic strain-to-fluctuation displacement operator. Instead of imposing 6 elementary loadings to solve the associated finite element boundary volume problems, one only needs to compute the localization-like operator $[\boldsymbol{M}]$ once with only considering the periodicity condition. Finally, substituting Eq. 5 into Eq. $2_{(2)}$, one obtains

$$\{\bar{\boldsymbol{\sigma}}\} = \left(\langle [\boldsymbol{C}] \rangle +^T [\boldsymbol{F}][\boldsymbol{M}] \right) \{\bar{\boldsymbol{\epsilon}}\} = [\boldsymbol{C}^*]\{\bar{\boldsymbol{\epsilon}}\}. \tag{6}$$

Obviously $[\boldsymbol{C}^*] = \langle [\boldsymbol{C}] \rangle +^T [\boldsymbol{F}][\boldsymbol{M}]$ is the effective (or homogenized) stiffness matrix. It is obtained with running only one finite element computation and with no need to compute the averaged fields of strains or stresses. The details of our approach as the main results are presented in [7].

3 Computational homogeneous properties

A reference model $\left(\rho^*/\rho^b = 6\%; t = 1; k = 1\right)$ (see Fig. 1) is generated with bulk properties (Young's modulus $E^b = 70\ GPa$, Poisson's ratio $\nu^b = 0.3$). In the next section, the influences of morphological parameters are carried out by comparing with the reference model.

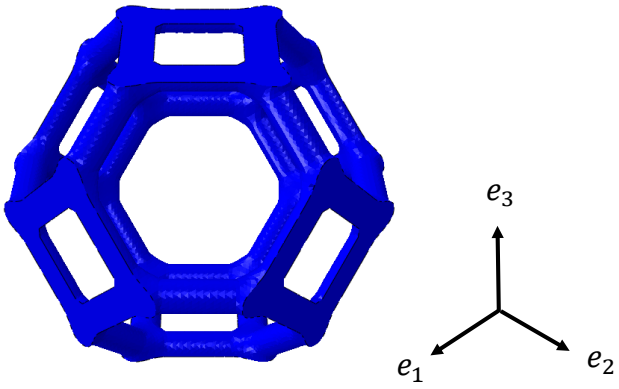

Figure 1 – The reference model $\left(\rho^*/\rho^b = 6\%; t = 1; k = 1\right)$

The result is more accurate when the mesh size is smaller (the number of elements is more). If the elements is infinitely many, the result will be infinitely close to the real value. With this conception,

[1] Variational Asymptotic Method for Unit Cell Homogenization

a linear relationship between the number of elements and the effective property could be generated to predict the convergence using the emprical criterion [9, 10]:

$$C_{ij}^{*} = C_{ij}^{0} + \frac{a}{N_e}, \tag{7}$$

where a is a constant and N_e stands for the number of elements.

When the reference model is meshed with 245006 elements using linear tetrahedral elements, the obtained effective elastic stiffness matrix in the frame (e_1, e_2, e_3) reads:

$$[\boldsymbol{C}^{*}] = \begin{bmatrix} 769.067 & 554.984 & 555.078 & 0 & 0 & 0 \\ & 768.740 & 554.944 & 0 & 0 & 0 \\ & & 768.690 & 0 & 0 & 0 \\ & & Sym & 80.994 & 0 & 0 \\ & & & & 80.963 & 0 \\ & & & & & 80.954 \end{bmatrix} (MPa).$$

One can see that there are only three independent components in the matrix, which makes the Kelvin foam effective behavior anisotropic with a cubic symmetry. Hence C_{11}^{*}, C_{12}^{*} and C_{44}^{*} are needed to derive the effective elastic properties. In order to present clearly, the relationship between C_{44}^{*} and the number of elements is plotted in Fig. 2 as example. The circular points are the computational results with different numbers of elements and the dashed fitting line is plotted based on Eq. 7 with the computational results. The value of the intersection point of this fitting line and Y axis, i.e. the triangular point in the figure, denotes the convergence result. The same mesh sensitivity analysis is done for the other effective components C_{12}^{*} and C_{44}^{*}. Finally, one obtains the symmetric cubic effective behavior illustrated in Table 3. This method is applied to all subsequent investigations.

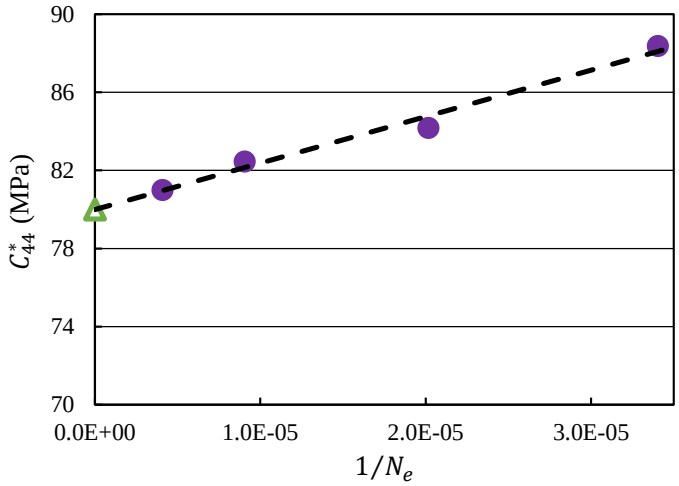

Figure 2 – Mesh sensitivity: dependency of C_{44}^{*} on the number of elements for the reference model $\left(\rho^{*}/\rho^{b} = 6\%, k = 1, t = 1\right)$

Table 3 – Converged effective behavior (cubic symmetry) for the reference model

$C_{11}^{*} = 765.373\ MPa$	$C_{12}^{*} = 555.698\ MPa$	$C_{44}^{*} = 79.994\ MPa$
$E^{*} = 297.873\ MPa$	$\nu^{*} = 0.421$	$G^{*} = 79.994\ MPa$

4 Influence of the morphological parameters on the effective behavior

4.1 Relative density

The model is assumed to have the morphological parameters $(t = 1; k = 1)$ and the relative density $\left(\rho^{*}/\rho^{b} = \{4\%; 6\%; 8\%; 10\%; 12\%; 14\%\}\right)$. Fig. 3 presents the evolutions of three effective elastic prop-

erties with the relative density. It could be observed that the variations of these effective properties caused by relative density are significant but different. With the increase of relative density, normalized property C^*_{12}/C^b_{12} rises linearly while C^*_{11}/C^b_{11} and C^*_{44}/C^b_{44} have quadratic increase.

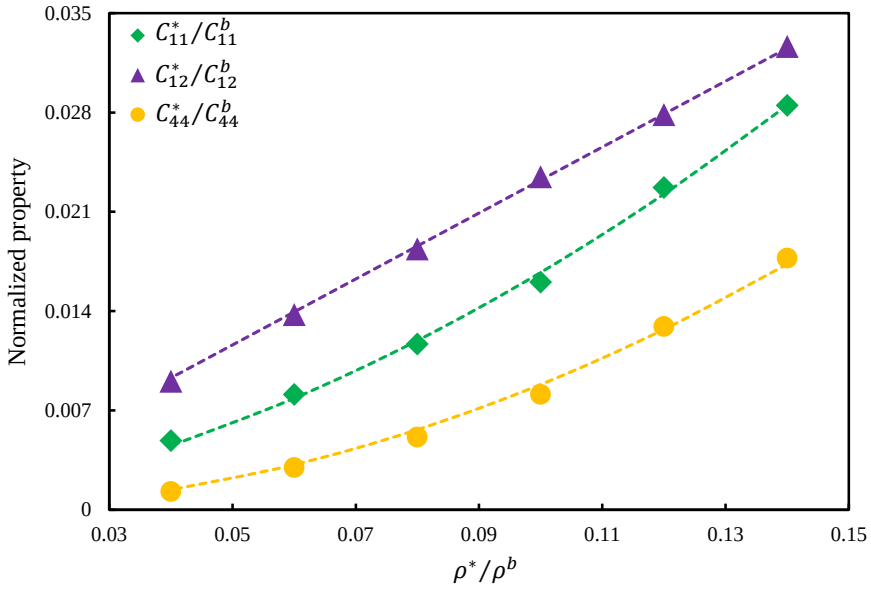

Figure 3 – Effect of the relative density on the normalized properties for the reference model $(t=1;k=1)$

The following equations with four coefficients $(\Phi_1;\Phi_2;\Phi_3;\Phi_4)$, are proposed to describe the relationship between the relative density and each effective property:

$$\begin{cases} \dfrac{C^*_{11}}{C^b_{11}} = \Phi_1\left(\dfrac{\rho^*}{\rho^b}\right)^2 + \Phi_2\left(\dfrac{\rho^*}{\rho^b}\right), \\ \dfrac{C^*_{12}}{C^b_{12}} = \Phi_3\left(\dfrac{\rho^*}{\rho^b}\right), \\ \dfrac{C^*_{44}}{C^b_{44}} = \Phi_4\left(\dfrac{\rho^*}{\rho^b}\right)^2. \end{cases} \tag{8}$$

The evolution of the morphological functions Φ_i is studied hereafter varying the different morphological parameters.

4.2 Diameter ratio

10 values in the range $[0.33,1]$ are selected as diameter ratios in order to be consistent with real foams. The investigation is performed on the models $\left(\rho^*/\rho^b = 6\%, k=1\right)$. The deviation indicator

$$e_{ij} = \frac{C^*_{ij} - C^{*0}_{ij}}{C^{*0}_{ij}},$$

is used to show the influence of diameter ratio on three effective properties clearly, where C^{*0}_{ij} stands for the corresponding property of the reference model $\left(\rho^*/\rho^b = 6\%, t=1, k=1\right)$. In Fig. 4, when the diameter ratio varies from 0.33 to 0.7, all three effective elastic properties have significant variations with the increase of diameter ratio. The variations of all three effective properties are much smaller in the range $(0.7,1]$, where the struts are flatter.

Four functions $\Phi_1(t)$, $\Phi_2(t)$, $\Phi_3(t)$ and $\Phi_4(t)$ are obtained for Kelvin open-cell foams with circular cross section struts by fitting with the computational results:

$$\begin{cases} \Phi_1(t) = 7.147t^3 - 16.885t^2 + 12.895t - 2.334, \\ \Phi_2(t) = 0.0114t + 0.0765, \\ \Phi_3(t) = -0.291t^2 + 0.518t + 0.00234, \\ \Phi_4(t) = 2.866t^3 - 7.496t^2 + 6.411t - 0.897. \end{cases} \tag{9}$$

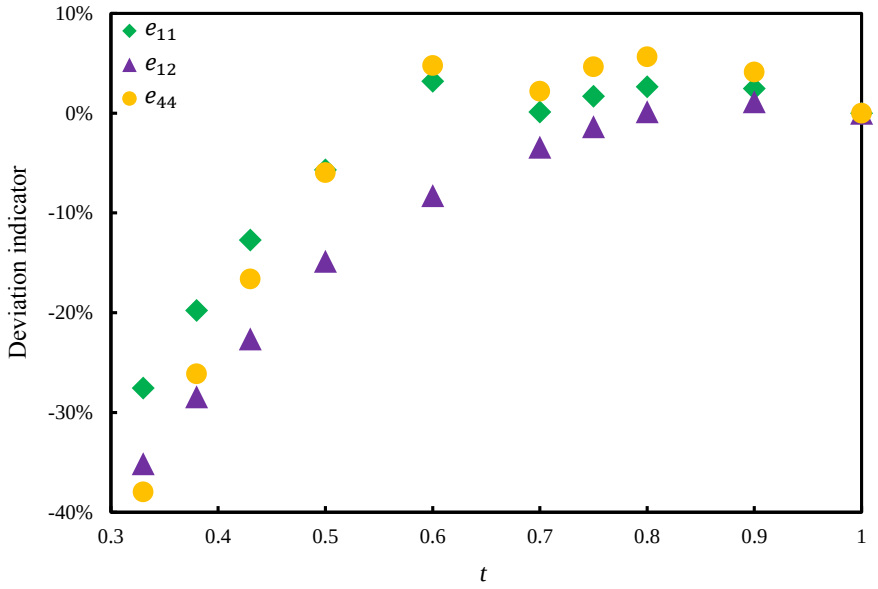

Figure 4 – Effect of the diameter ratio on the deviation indicators for the models $\left(\rho^*/\rho^b = 6\%, k = 1\right)$

The agreements between the analytic laws (Eq. 9) and the computational results are considered satisfying. The mean relative errors of C^*_{11}/C^b_{11}, C^*_{12}/C^b_{12} and C^*_{44}/C^b_{44} are 2.47%, 1.75% and 3.04% respectively.

4.3 Normalized curvature

The influence of normalized curvature is studied while k varies within $[-0.3, 1]$. The investigation is carried out using the models $\left(\rho^*/\rho^b = 6\%, t = 1\right)$. In Fig. 5, one could see that the variation of e_{12} is very small, which means the influence of normalized curvature on C^*_{12} is negligible throughout the whole range. In the range $[-0.3, 0.25]$, the influence of normalized curvature is significant for e_{11} and e_{44}, especially for e_{44}. Whereas the variations of e_{11} and e_{44} are relatively much smaller in the range$(0.25, 1]$.

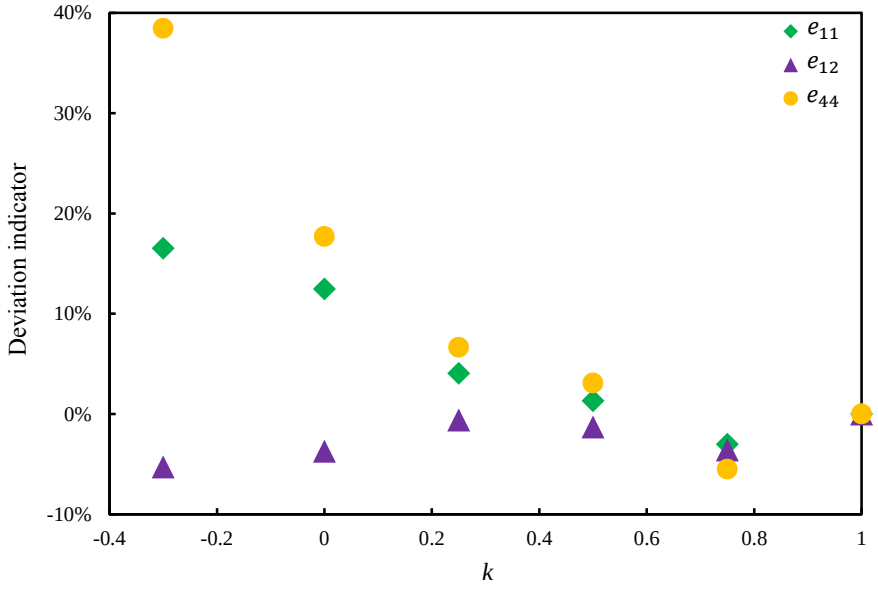

Figure 5 – Effect of the normalized curvature on the deviation indicators for the models $\left(\rho^*/\rho^b = 6\%, t = 1\right)$

Similarly, four linear functions $\Phi_1(k)$, $\Phi_2(k)$, $\Phi_3(k)$ and $\Phi_4(k)$ are obtained for Kelvin open-cell

foams with constant diameter struts by fitting:

$$\begin{cases} \Phi_1(k) = -0.135k + 1.009, \\ \Phi_2(k) = -0.0122k + 0.091, \\ \Phi_3(k) = 0.0116k + 0.222, \\ \Phi_4(k) = -0.179k + 1.045. \end{cases} \tag{10}$$

The mean relative errors of C^*_{11}/C^b_{11}, C^*_{12}/C^b_{12} and C^*_{44}/C^b_{44} are 2.06%, 1.95% and 6.08% respectively.

5 Conclusion

A new model is proposed to generate Kelvin open-cell structure by taking into account a number of morphological parameters, including the shape of cross section of strut and the cross-sectional area of a strut along the strut axis. A periodic Hill's lemma computational homogenization approach, inspirated from the VAMUCH method, is used to analyse the influences of these morphological parameters on effective elastic properties. New generic laws are proposed to predict the effective elastic properties of Kelvin open-cell foam. The complete results are shown in [7].

References

[1] R. Coquard, D. Baillis. *Modeling of heat transfer in low-density eps foams*. J. Heat Trans, 128, 538-549, 2006.

[2] A. Iluk. *Global stability of an aluminum foam stand-alone energy absorber*. Archives of Civil and Mechanical Engineering, 13, 137-143, 2013.

[3] A. Düster, H.G. Sehlhorst, E. Rank. *Numerical homogenization of heterogeneous and cellular materials utilizing the finite cell method*. Computational Mechanics, 50, 413-431, 2012.

[4] P.M. Suquet. *Elements of Homogenization for Inelastic Solid Mechanics*. Springer Berlin Heidelberg, Berlin, Heidelberg, 193-278, 1987.

[5] H. Moulinec, P. Suquet. *A numerical method for computing the overall response of nonlinear composites with complex microstructure*. Computer Methods in Applied Mechanics and Engineering, 157, 69-94, 1998.

[6] W. Yu, T. Tang. *Variational asymptotic method for unit cell homogenization of periodically heterogeneous materials*. International Journal of Solids and Structures, 44, 3738-3755, 2007.

[7] W. Zhu, N. Blal, S. Cunsolo, D. Baillis. *Micromechanical modeling of effective elastic properties of open-cell foam*. (accepted by International Journal of Solids and Structures), 2017.

[8] J. Storm, M. Abendroth, M. Kuna. *Numerical and analytical solutions for anisotropic yield surfaces of the open-cell kelvin foam*. International Journal of Mechanical Sciences, 105, 70-82, 2016.

[9] A.P. Roberts, E.J. Garboczi. *Elastic properties of model porous ceramics*. Journal of the American Ceramic Society, 83, 3041-3048, 2000.

[10] J.M. Gatt, Y. Monerie, D. Laux, D. Baron. *Elastic behavior of porous ceramics: application to nuclear fuel materials*. Journal of Nuclear Materials, 336, 145-155, 2005.